INT. J. REMOTE SENSING, 2002, VOL. 23, NO. 8, 1639–1661

A five channel chlorophyll concentration algorithm applied to SeaWiFS data processed by SeaDAS in coastal waters

F. GOHIN

IFREMER Centre de Brest, BP 70—29280 Plouzane, France;
e-mail: Francis.Gohin@ifremer.fr

J. N. DRUON

EU—Joint Research Centre, Space Applications Institute, TP 442,
I-21020 Ispra (VA), Italy

L. LAMPERT

EPSHOM/CMO/CM BP 30316—29603 Brest Cédex, France

(*Received 2 May 2000; in final form 26 March 2001*)

Abstract. Chlorophyll-a concentration derived from the Sea-viewing Wide Field-of-view Sensor (SeaWiFS) after applying the current SeaWiFS Data Analysis System (SeaDAS) processing tools appears to be higher than reality in coastal areas, particularly from late summer to early spring when optical properties of water are dominated by yellow substances and suspended matter. As a complement to the SeaWiFS standard procedure addressing clear water, empirical algorithms can bring immediate progress for observing the coastal domain. This paper proposes to modify the SeaWiFS Ocean Colour 4 band algorithm (OC4) by including the 412 and 555 channels. The effect of the suspended matter on the ratios used as inputs in OC4 is revealed by the 555 channel whereas the atmospheric over-correction and the absorption by yellow substances are related to the 412 channel. Based on a dataset located in the English Channel and on the continental shelf of the Bay of Biscay, a parametrization of the relationship between the OC4 ratio and the 412 and 555 bands has been empirically proposed for different chlorophyll concentrations. Application of a lookup table, relating triplets (OC4 band ratio, 412 and 555 bands) to chlorophyll-a concentration, provides realistic concentration maps likely to satisfy the needs of researchers involved in environmental surveying or fishery management.

1. Introduction

The first goal of ocean colour algorithms from a space sensor such as the Sea-viewing Wide Field-of-view Sensor (SeaWiFS) is to provide global surface chlorophyll-a concentrations (Hooker *et al.* 1992) in order to complement the dataset which began in the late 1970s with the Coastal Zone Colour Scanner (CZCZ) aboard NIMBUS 7 (from October 1978 to June 1986). Such a global series will be of great use for studying long-term trends in oceanic production and carbon recycling. A higher accuracy in chlorophyll concentration is obtained in clear water, defined as case 1 water according to the optical classification proposed by Morel and Prieur

International Journal of Remote Sensing
ISSN 0143-1161 print/ISSN 1366-5901 online © 2002 Taylor & Francis Ltd
http://www.tandf.co.uk/journals
DOI: 10.1080/01431160110071879

(1977). In case 1 water, the optical properties are dominated by chlorophyll and associated degradation products. In coastal waters, classified as case 2, suspended particulate sediments and yellow substances from terrestrial origin, which are not co-varying with chlorophyll-a concentration, dramatically increase the errors in chlorophyll concentration estimates (Carder *et al.* 1991). However, a large community of biologists, involved in fishery research or coastal ecology, is waiting for chlorophyll-a concentration maps provided by space sensors comparable to the results of their cruises or the outputs of their numerical models.

Since its launch in September 1997, SeaWiFS has been providing images which can be easily processed thanks to the free access software, SeaWiFS Data Analysis System (SeaDAS) (Fu *et al.* 1998), provided by NASA.

For coastal waters, the main problems appearing in SeaWiFS level 2 products are frequent negative water-leaving radiances in the short wavelengths and too high chlorophyll-a concentrations. Negative values of radiance can be attributed to an over-estimation of the aerosol contribution which is subtracted from the total signal. This effect is therefore particularly apparent in areas where, due to high concentration of coloured dissolved organic matter (CDOM), also called gelbstoff, the water-leaving radiance is naturally low at short wavelengths. The assessment of the aerosol contribution to the total radiance is obtained at any wavelength by extrapolating the signal observed in the near-infrared domain where the water radiance is low. In coastal areas, two effects contribute to reduce the efficiency of a standard atmospheric correction working by extrapolation. The first one is known as the 'bright pixel' effect. In the case of 'bright pixels', whitish particles from terrestrial origin and plankton associated particles enhance the infrared radiance which can no more be attributed to the atmosphere alone. Recent improvement has been obtained in SeaDAS 4.0 (Siegel *et al.* 2000) by introducing the contribution of the plankton itself, through the particulate backscattering coefficient, to the near-infrared radiance. However, the concepts developed in the current version of the software, dedicated to case 1 water, are based only on the contributions of the atmosphere (through standard aerosol models) and plankton, ignoring any effect of CDOM or particles from terrestrial origin. Details on the 'bright pixel' effect and the way to cope with it in the case of a multi infrared channel sensor such as the Medium Resolution Imaging Spectrometer (MERIS), can be found in Moore *et al.* (1999). The second cause of error in the standard atmospheric correction can be attributed to the particular characteristics of the coastal atmosphere which can be different from any of the conventional types included in the SeaDAS reference set. The error sources in the atmospheric correction from the Moderate Resolution Imaging Spectrometer (MODIS) are discussed in Gordon (1999). Negative values are not by themselves a problem as the short wave channels are not used in the OC4 SeaDAS default algorithm (switching from 443 to 510 nm for coastal data) but they are a warning that the atmospheric contribution to the total reflectance is over-estimated, leading to erroneous water-leaving radiances at any wavelength.

In specific atmospheres, for instance when absorbing aerosols are present, Gordon *et al.* (2000) propose a new approach to the atmospheric correction, based on a single-step process, retrieving simultaneously atmosphere and water properties. In coastal waters, however, the complexity of the aerosol nature, linked to the wind direction, and the variability of water composition in suspended matter, CDOM and pigment types, multiply the number of unknown parameters in the modelling of the radiative transfer. For those reasons, and considering that many teams are already

developing analytical algorithms, particularly dedicated to MODIS and MERIS, our study has focused on a simple empirical and regional algorithm to provide chlorophyll concentration in the English Channel and in the Bay of Biscay from the SeaWiFS radiances processed by SeaDAS in its current 4.0 version. In contrast to other promising methods modifying the default SeaDAS procedure by selecting manually clear water areas to get information on the atmosphere (Hu *et al.* 1998), we will use the radiances as they result from the current algorithm. Thus, the chlorophyll concentrations will be estimated from an empirical algorithm which accepts negative radiances as input data.

2. The ocean colour algorithms

The remote sensing reflectance $R_{rsw}(\lambda)$ of water at wavelength, λ, is the key parameter used in the ocean colour algorithms. It can be defined as:

$$R_{rsw}(\lambda)=\frac{\pi L_w(\lambda)}{E_d} \tag{1}$$

where $L_w(\lambda)$ is the water-leaving radiance and E_d is the downwelling solar irradiance just above the sea surface. In satellite remote sensing theory, E_d is commonly modelled by $t_0(\lambda)F_0(\lambda)\cos(\theta_0)$ where $F_o(\lambda)$ is the extraterrestrial solar irradiance, $t_0(\lambda)$ the diffuse transmittance of the atmosphere in the solar direction, and θ_0 the solar zenith angle.

In equation (1), πL_w is an approximation of the upward radiance. Such an approximation is questionable in coastal waters as the light is not totally diffuse. As a matter of fact, L_w is dependent on the viewing geometry and the solar position in a way which is not easily determined in coastal waters. For that reason, the most efficient ocean colour algorithms use radiance ratios which eliminate partly these effects, varying slowly with the wavelength. In building a new algorithm to circumvent this problem, we have to take care to use radiance ratios or water-leaving radiances L_w, defined simultaneously at two or more wavelengths.

2.1. *Analytical and semianalytical algorithms*

In the analytical approach, radiative transfer theory provides a relationship between upwelling radiance and the inherent optical properties of the water (Sathyendranath and Platt 1997).

$$R_{rsw}(\lambda)=\alpha\frac{t^2R(\lambda)}{[1-rR(\lambda)]n^2} \tag{2}$$

where α is weakly dependent upon λ and θ_0, $R(\lambda)$ is the irradiance reflectance defined through $E_u(0^-)=R(\lambda)E_d(0^-)$, where $E_u(0^-)$ and $E_d(0^-)$ are respectively the upwelling and downwelling irradiance just beneath the surface, t is the transmittance of the air–sea interface, n is the real part of the index of refraction of sea water, and r is the air-water reflectance for diffuse irradiance. As noticed by Moore *et al.* (1999) the term $1-rR(\lambda)$, normally assumed to equal 1 for case 1 waters, has to be considered with care for waters laden with sediments of high reflectance.

R is function of the inherent optical properties of sea water.

$$R(\lambda)\approx\frac{\beta b_b(\lambda)}{a(\lambda)+b_b(\lambda)} \tag{3}$$

where a and b_b are the absorption and backscattering coefficients.

Both parameters can be expanded as a sum:

$$a(\lambda)=a_{\mathrm{w}}(\lambda)+a_{\phi}(\lambda)+a_{\mathrm{spm}}(\lambda)+a_{\mathrm{g}}(\lambda) \tag{4}$$

where the subscripts w, ϕ, spm, and g refer to water, phytoplankton, suspended particulate matter and gelbstoff.

The formula for the backscattering coefficient $b_{\mathrm{b}}(\lambda)$ is simpler, and $b_{\mathrm{b}}(\lambda)$ is expanded as:

$$b_{\mathrm{b}}(\lambda)=b_{\mathrm{w}}(\lambda)+b_{\mathrm{bp}}(\lambda) \tag{5}$$

where p refers to particles.

In open ocean, $b_{\mathrm{b}}(\lambda)$ is usually much smaller than $a(\lambda)$ and thus can be removed from the denominator of equation (3):

$$R_{\mathrm{rsw}}(\lambda)\approx \frac{\gamma b_{\mathrm{b}}(\lambda)}{a(\lambda)} \tag{6}$$

However, in green coastal water, Carder *et al.* (1993) noticed that, for an absorption coefficient of $0.07\,\mathrm{m}^{-1}$ or less, a backscattering coefficient value of as little as $0.01\,\mathrm{m}^{-1}$ becomes significant.

In fact, most of the algorithms are called semi-analytical as different empirical expressions or simplifications are proposed to approximate the spectral shapes of the terms *a* and *b*. These semi-analytical algorithms are particularly suited for MERIS and MODIS as they take advantage of their numerous channels to calculate the bio-optical parameters. Carder *et al.* (1999) propose a MODIS ocean colour algorithm relating the reflectances R_{rsw} to three unknowns: one constant term, $a_{\phi}(675)$, and $a_{\mathrm{g}}(400)$. To invert their R_{rsw} model equations, they use the spectral reflectance ratios $R_{\mathrm{rsw}}(412)/R_{\mathrm{rsw}}(443)$ and $R_{\mathrm{rsw}}(443)/R_{\mathrm{rsw}}(551)$. For waters with high concentration of gelbstoff and chlorophyll, the reflectance values $R_{\mathrm{rsw}}(412)$ and $R_{\mathrm{rsw}}(443)$ are small and the algorithm does not perform as well as in clear waters. In such areas, the authors propose to use a standard empirical algorithm, similar to OC4. Thus, for case 2 water, whatever the ocean colour algorithm used, analytical or semi-analytical, the first condition is to get accurate marine reflectances, particularly in the lower wavelengths, which can only be provided through efficient and adapted atmospheric corrections.

2.2. *Empirical algorithms*

In oligo- and meso-trophic waters, the chlorophyll-a and its co-varying derived products are considered to be the main contributors to the water reflectance. A simple relationship, with a sigmoid shape, links the log-transformed reflectance ratios to chlorophyll-a concentrations.

$$\textbf{\textit{OC2}}\ \text{Chl-a}=10^{(0.319-2.336R+0.879R^2-0.135R^3)}-0.071 \tag{7}$$

where $R=\log 10(R_{\mathrm{rsw}}(490)/R_{\mathrm{rsw}}(555))$.

Since CZCS, most pigment estimates are derived from switching algorithms. In Gordon *et al.* (1980), the blue-green ratio $R_{\mathrm{rsw}}(443)/R_{\mathrm{rsw}}(550)$ is used for concentrations below 1 or $1.5\,\mu\mathrm{g}\,\mathrm{l}^{-1}$ and the ratio $R_{\mathrm{rsw}}(520)/R_{\mathrm{rsw}}(550)$ above this threshold, when the former band ratio is too low. There are two major reasons for the success of the switching algorithms. In coastal water, the contribution of CDOM to the blue-green ratio is comparable or superior to that of phytoplankton pigments (Carder

et al. 1991) and, because the signal is very low, signal to noise ratio increases for small wavelengths.

In the review of chlorophyll algorithms for SeaWiFS by O'Reilly *et al.* (1998), the OC4 switching algorithm yielded one of the best results after tuning to a common dataset.

The OC4 algorithm uses a single set of coefficients applied to the ratio R_G which is determined by the greatest ratio among $R_{rsw}(443)/R_{rsw}(555)$, $R_{rsw}(490)/R_{rsw}(555)$, and $R_{rsw}(510)/R_{rsw}(555)$.

For R equal to $\log_{10}(R_G)$:

$$\textbf{\textit{OC4}}\ \text{Chl-a} = 10^{(0.366 - 3.067R + 1.93R^2 + 2.649R^3 - 1.532R^4)} - 0.0414 \tag{8}$$

OC2 and OC4 formulations and coefficients are obtained from SeaDAS4.0 documentation.

3. Estimation of the water remote sensing reflectance from space data

3.1. *The atmospheric correction*

Before any use of the marine reflectance ratios in an ocean colour algorithm as OC2 or OC4, an accurate atmospheric correction has to be made as it is well known that the contribution arising from aerosol scattering is dominant (up to 80%) in the radiance reaching the sensor. The total reflectance R_t measured at the top of the atmosphere, defined by $R_t = \pi L(\lambda)/F_0(\lambda)\cos(\theta_0)$, where L is the satellite sensed radiance, can be divided into three components.

$$R_t \approx R_r(\lambda) + R_{as}(\lambda) + t_v(\lambda)t_o(\lambda)R_{rsw}(\lambda) \tag{9}$$

where:

- $R_r(\lambda)$ is the Rayleigh component due to the scattering by air molecules
- $R_{as}(\lambda)$ is the reflectance due to the aerosol scattering
- $t_v(\lambda)$ is the diffuse transmittance of the atmosphere from the sea to the sensor.

$t_v(\lambda) = e^{\{-(\tau_r/2 + \tau oz)/\cos(\theta)\}}$ where τ_r is the Rayleigh optical thickness, and τ_{oz} is the ozone optical thickness at wavelength λ, θ is the zenith angle from the pixel to the sensor.

From Gordon and Wang (1994), we can write $R_{as}(\lambda)$ as:

$$R_{as}(\lambda) = \tau_a(\lambda)\omega_a(\lambda)p_a(\theta, \theta_0, \lambda)/4\cos(\theta)\cos(\theta_0) \tag{10}$$

$\tau_a(\lambda)$ is the aerosol optical thickness, $\omega_a(\lambda)$ the aerosol single scattering albedo, p_a is the aerosol scattering phase function.

From equation (9) we derive: $R_{rsw}(\lambda) = [R_t - R_r(\lambda) - R_{as}(\lambda)]/t_v(\lambda)t_o(\lambda)$ where $R_{as}(\lambda)$ is unknown.

To determine $R_{as}(\lambda)$ at any λ, the values of R_{as} are calculated at 765 and 865 nm where R_{rsw} is assumed to be zero. Then, $R_{as}(\lambda)$ is assessed at any λ thanks to the parameter $\varepsilon(\lambda, 865)$:

$$R_{as}(\lambda) = \varepsilon(\lambda, 865)R_{as}(865) \tag{11}$$

$\varepsilon(\lambda, 865)$ being approximated by $e^{c(\lambda - 865)}$ where c depends on the model and the viewing geometry.

Actually, in the SeaWiFS, MERIS (Antoine and Morel 1999) and MODIS

algorithms, the model described in equation (8), used for CZCS, is modified to take into account multiple scattering.

$$R_{as}(\lambda) = R_a(\lambda) + R_{ra}(\lambda)$$

where $R_a(\lambda)$ is the reflectance resulting from multiple scattering by aerosols in the absence of air. $R_{ra}(\lambda)$ results from interactions between aerosol and molecular scattering. Multiple scattering effects are particularly enhanced in areas of high aerosol optical thickness and in the case of absorbing particles, e.g. in regions with a strong continental influence.

3.2. *The performance of the atmospheric correction algorithm*

The atmospheric correction is still a task under investigation and development. Several aspects, considered as minor in preliminary algorithms, are now examined with care. The effect of absorption by O_2 at 759 nm on the retrieved $\varepsilon(765, 865)$, the contribution of the wind driven white caps to the signal are not negligible problems. However, in coastal areas, the performance of the atmospheric correction, measured by $\Delta R_{rsw}(\lambda)$, is particularly low owing to the fact that the aerosol types may be distinct from any of the conventional atmosphere models included in the reference set, and that the water-leaving radiance is far from being negligible in the near-infrared domain (765–865 nm).

From equation (9), one obtains $\Delta R_{rsw}(\lambda) = -\Delta\varepsilon(\lambda, 865) R_{as}(865)/t_t$, where t_t is equal to $t_v(\lambda)t_o(\lambda)$, and from equation (10)

$$\Delta R_{rsw}(\lambda) = -\Delta\varepsilon(\lambda, 865)\tau_a(865)\omega_a(\lambda)p_a(\theta, \theta_0, 865)/4\cos(\theta)\cos(\theta_0)t_t) \qquad (12)$$

From figure 1, it appears that coastal models with low humidity lead to high $\varepsilon(\lambda, 865)$ and thus to high $\Delta\varepsilon(\lambda, 865)$. For maritime aerosols, $\varepsilon(\lambda, 865)$, close to one, shows little evolution with λ. Furthermore, $\Delta R_{rsw}(\lambda)$ is proportional to $\tau_a(865)$ which reaches its lowest levels (≈ 0.1) in the open ocean, far from any source of pollution and/or desert aerosols. In areas subject to urban pollution, high optical thicknesses are likely to occur.

In case 2 waters, the water reflectance in the near-infrared is not zero and the estimate of $\varepsilon(765, 865)$, $\varepsilon^*(765, 865)$, is not purely atmospheric.

$$\varepsilon^*(765, 865) = \frac{R_{as}(765) + t_t R_{rdw}(765)}{R_{as}(865) + t_t R_{rsw}(865)}$$

$$\varepsilon^* \simeq \varepsilon + t_t[R_{rsw}(765)/R_{as}(865) - R_{as}(765)R_{rsw}(865)/R_{as}(865)^2\}$$

which becomes

$$\varepsilon^* \simeq \varepsilon + t_t R_{rsw}(765)/R_{as}(865)[1 - \varepsilon R_{rsw}(865)/R_{rsw}(765)] \qquad (13)$$

Referring to Moore *et al.* (1999), the quantity $R_{rsw}(865)/R_{rsw}(765)$ can reach 0.5 (low sediment loads) and 0.9 (high sediment loads), leading to a positive term $\{1 - \varepsilon R_{rsw}(865)/R_{rsw}(765)\}$ if ε is close to one. The term $R_{rsw}(765)$ is very sensitive to the backscattering coefficient of sediment, which, for whitish suspended sediment particles, is still high at 765 nm.

Based on a bio-optical modelling of the reflectance as a function of chlorophyll concentration, Siegel *et al.* (2000) show that the over-estimation of the atmospheric effects is also significant in the case of productive water. Taking into account their results, an iterative procedure is used in SeaDAS 4.0 to estimate alternatively the

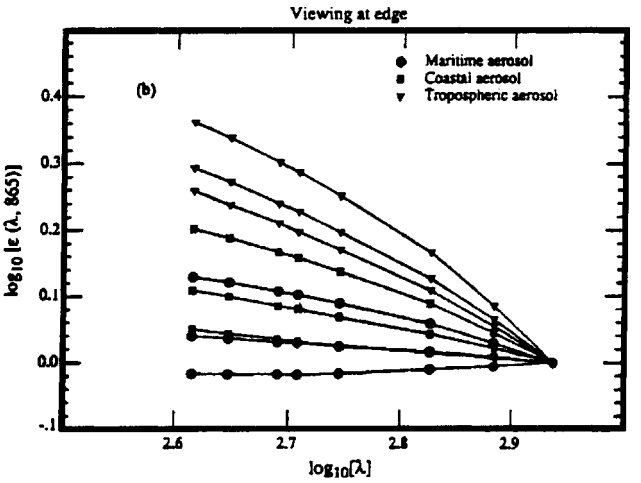

Figure 1. $\varepsilon(\lambda, 865)$ as a function of λ for viewing at the edge with $\theta_0 = 60^\circ$ for the maritime, coastal and tropospheric aerosol models. For each model, the relative humidity values are 70, 90 and 98% from the upper to the lower curves (from Gordon and Wang 1994).

aerosol and water components of the total reflectance in the near-infrared domain. However, this correction does not account for the effects of sediments.

3.3. *Qualitative assessment of the water-leaving radiances derived from a standard processing scheme in coastal waters*

A qualitative assessment of the main sources of errors encountered in a standard processing scheme retrieving water-leaving radiances from radiances measured at sensor can be proposed for coastal waters. Without making an exhaustive list of the elementary processes occurring in the radiative path, we can emphasize the following points, departing from mean calibration conditions, encountered in temperate and coastal seas, from the plankton cells to the top of atmosphere:

3.3.1. *Packaged/Unpackaged cells*

It is known (Morel and Bricaud 1981) that the absorption coefficient of phytoplankton $a_\phi(\lambda)$ is inversely related to the cell size for a given pigment concentration. As noted by Carder *et al.* (1991), since tropical and subtropical phytoplankon cells are typically smaller ('unpackaged' pigments) than those from temperate and boreal regions ('packaged' pigments), we can expect in our data, for a given pigment concentration, reflectances higher than those measured in the reference calibration data which are mainly tropical and subtropical.

3.3.2. *High contents in degradation products and suspended particulate sediments*

In contrast, an increase in CDOM not co-varying with the true pigment concentration will reduce the upwelled radiances in the blue, leading to an over-estimation of the chlorophyll concentration. The CDOM from terrestrial origin induces a decrease of the mean reflectances at short wavelengths, hence an over-estimation of the chlorophyll concentration. Moreover, the CDOM-to-chlorophyll ratio, depending on the physiological state of the phytoplankton, can change very quickly in coastal areas leading to over or under-estimation of the pigment concentration. Nevertheless, the terrestrial CDOM contributes to a mean over-estimation of the chlorophyll concentration in coastal waters. In such waters, laden in suspended

particulate sediments and detritus, an increase in scattering is observed, depressing the reflectance ratios and, hence, increasing again the retrieved concentration of chlorophyll.

3.3.3. *An over-estimation of the atmospheric component*

We have already noticed that coastal aerosols may differ from those modelled in the standard dataset. The exponential dependency of ε is critical and not verified in coastal and tropospheric models, particularly for the smallest wavelengths. Nevertheless, the dominant error term is due to the residual water-leaving radiances of coastal waters, laden in suspended particulate matters, in the near-infrared, making questionable the basic hypotheses of the atmospheric correction algorithm. An over-estimation of the atmospheric content is therefore likely to occur in coastal waters. Negative water-leaving radiances are often derived from the application of a standard ocean colour algorithm defined for case 1 data. This effect is very apparent on the images as the natural radiances are low at short wavelengths.

Figure 2 shows different errors leading to negative radiances in coastal water. It must be noted that the processes (absorption by CDOM, backscattering by suspended particles) involved in the alteration of the reflectance ratios are not independent in coastal waters.

4. The *in situ* dataset and the SeaWiFS scenes

4.1. *The* in situ *dataset*

In order to adapt our model to the coastal domain, a threshold of $0.2\,\mathrm{mg\,m^{-3}}$ is applied to the *in situ* concentrations. From January 1998 to June 2000, we obtained a set of 178 'coincident and clear' pairs of data, 56 in the English channel, most of them located in the Bay of Seine, and 122 in the Bay of Biscay (tables A1, A2, A3 and figure 3). *In situ* and clear satellite data are considered as coincident when they are observed on the same day. The time shift between satellite and field measurements does not exceed 12 h for coastal (or in plumes) stations and 36h for stations where the time variability is lower. The in situ data range from 0.2 to $44\,\mathrm{mg\,m^{-3}}$. Their mean is equal to $3.27\,\mathrm{mg\,m^{-3}}$ (see tables A1 and A2 for details).

4.2. *The satellite dataset*

The basic satellite data are normalized water-leaving radiances (table A3) obtained from NASA and processed with SeaDAS version 4.0.

The normalized water-leaving radiance calculated by SeaDAS was defined by Gordon and Clark (1981) through: $L_w = L_w(\lambda)_N \cos(\theta_0) t_0(\lambda)$.

$$L_w = L_w(\lambda)_N \cos(\theta_0)\, e^{\{-(\tau r/2 + \tau oz)/\cos(\theta_0)\}} \tag{14}$$

The normalized water-leaving radiance $L_w(\lambda)_N$ is approximately the radiance that would exit the ocean in the absence of the atmosphere, the sun being at the zenith.

$L_w(\lambda)_N$ is related to R_{rsw}, as defined in equation (1), by

$$R_{rsw} = \frac{\pi L_w(\lambda)_N}{F_0(\lambda)} \tag{15}$$

From equations (1) and (15), the spectral ratios used in OC2 or OC4 can be expressed as:

$$\frac{R_{rsw}(\lambda_1)}{R_{rsw}(\lambda_2)} = \frac{L_w(\lambda_1)_N F_0(\lambda_2)}{L_w(\lambda_2)_N F_0(\lambda_1)} \tag{16}$$

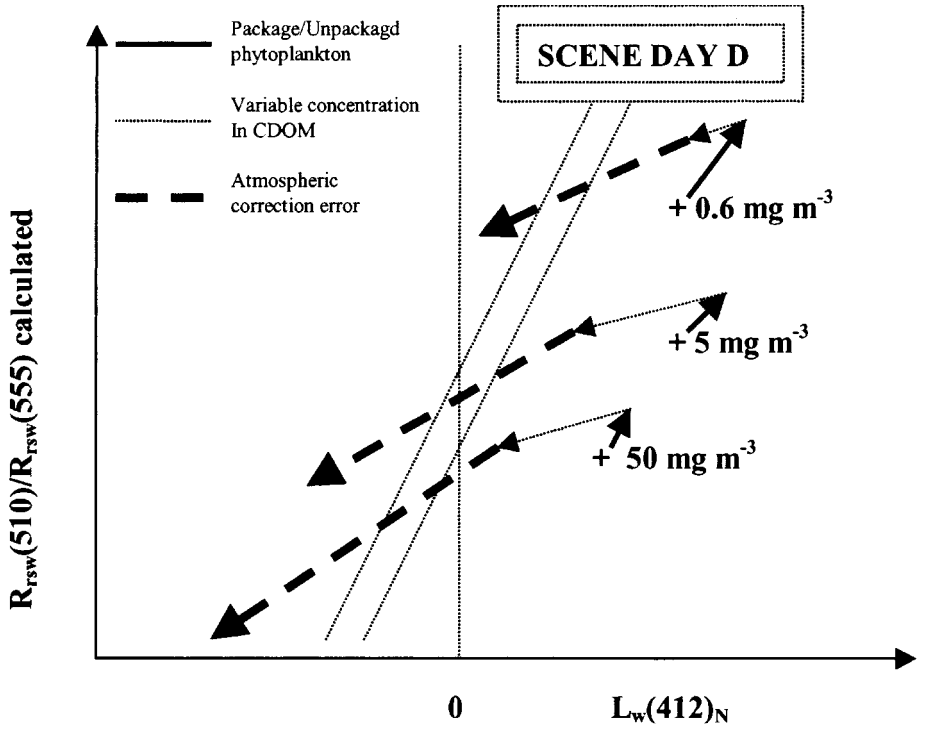

Figure 2. Schematization of the main terms of error leading to biased results in the band ratio and the radiance at 412 nm when applying a case 1 algorithm to coastal data. In the ($R_{rsw}(510)/R_{rsw}(555)$, $L_w(412)_N$) space, crosses, +, indicate the mean positions of field measurements for case 1 water. The cumulated errors lead to a decrease in the reflectance ratios and an over-estimation in chlorophyll-a concentration. For a SeaWiFS scene observed at day D over a region subject to homogeneous error terms (physiological states of phytoplankton, CDOM, sediment, atmosphere), the biases are not independent from one pixel to another.

5. The OC2 and OC4 algorithms applied to SeaWiFS data processed by SeaDAS

Applying OC2 and OC4 algorithms to SeaDAS data over-estimates the chlorophyll concentrations (figures 4 and 5) in relatively chlorophyll-poor waters, where the relative part of the suspended matter and the yellow substances in the optical properties of water is high. For such waters, benefit in accuracy by using one algorithm or the other seems negligible compared with the biases and the noises. However, we have chosen the OC4 band ratio as it is recommended in the literature for a larger variety of waters, including chlorophyll rich waters. Two negative OC2 ratios $R_{rsw}(490)/R_{rsw}(555)$ and one negative ratio OC4 have been observed for our dataset. The cumulative relative frequency distributions of the maximum band ratios, shown in figure 4(*c*), are similar to what was expected from the literature (O'Reilly *et al.* 1998) although we observe a switch of the cumulative frequency curves towards lower *in situ* chlorophyll concentrations. All these observations confirm that our satellite data, processed by OC4, behave as if they were related to chlorophyll concentrations higher than reality, particularly when the measured concentration is lower than 10 mg m^{-3}.

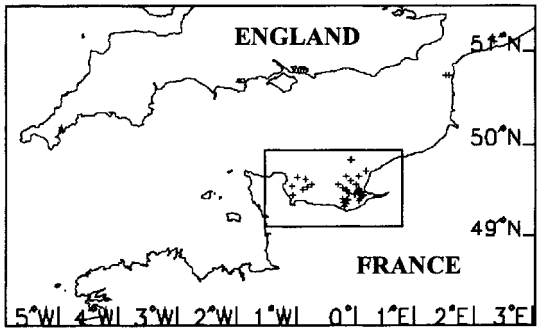

(a) Locations of the Channel data. Most of the data are in the Bay of Seine (region within the box)

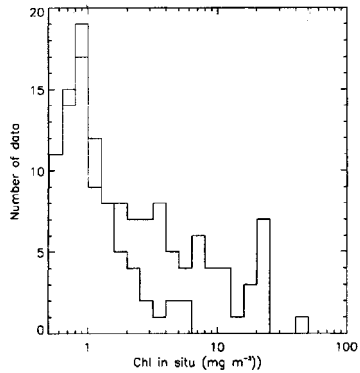

(c) Distribution of Chl *a* concentrations in the total data set (upper histogram) or Bay of Biscay data set (lower histogram)

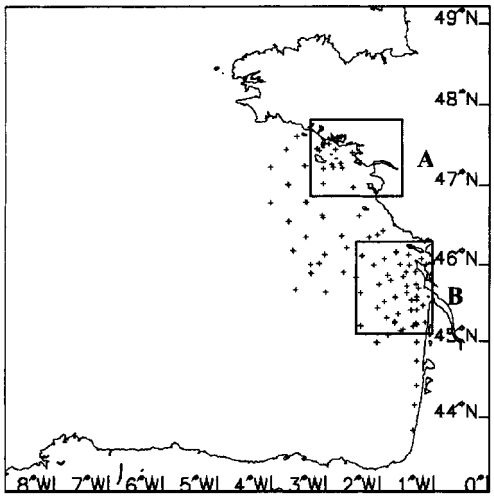

(b) Locations of the Bay of Biscay data set
A Vilaine-Loire region, **B** Gironde region

Figure 3. Data distribution in the English Channel and the Bay of Biscay. (*a*) Locations of the Channel data. Most of the data are in the Bay of Seine (region within the box). (*b*) Locations of the Bay of Biscay dataset A Vilaine-Loire region, B Gironde region. (*c*) Distribution of chlorophyll a concentrations in the total dataset (upper histogram) or Bay of Biscay dataset (lower histogram).

6. The modified OC4 algorithm

6.1. *Modelling the OC4 band ratio behaviour in a 3-dimensional space*

In our procedure, the chlorophyll concentration is determined from the triplet (OC4 maximum band ratio, $L_w(412)_N$, $L_w(555)_N$). To build a lookup table relating a SeaWiFS pixel, characterized by its position in this 3-dimensional space, to chlorophyll concentration, we proceed in three steps. First, the positions of eleven iso-concentration lines C_I, from 0.2 to 65 mg m^{-3}, are parametrized in the plane $L_w(555)_N = 0$. Second, iso-concentration surfaces, departing from these iso-lines, are generated in the 3-dimensional space. The iso-surfaces are drawn assuming

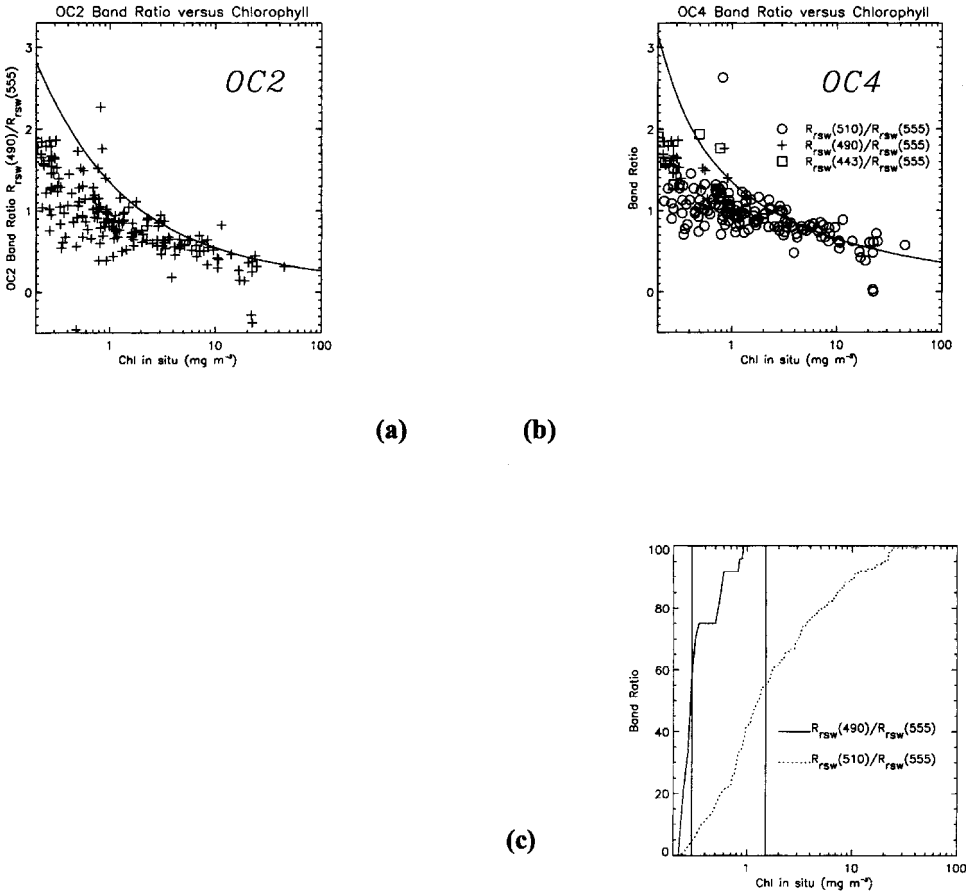

Figure 4. SeaWiFS band ratios (+) versus *in situ* chlorophyll a concentration. (*a*) OC2 band ratios and theoretical curve, (*b*) OC4 band ratios and theoretical curve, (*c*) cumulative relative frequency distribution of maximum band ratios; (*c*) presents the 0.3 and 1.5 mg m^{-3} axes which are supposed, from *in situ* measurements found in the literature, to bracket the $R_{rsw}(490)/R_{rsw}(555)$ ratio. The general behaviour of the SeaDAS band ratios is similar to what would have been observed for chlorophyll concentrations higher than those measured.

an exponential decrease as a function of $L_w(555)_N$. Third, on a regular 3-D grid, values of chlorophyll concentrations are calculated by interpolation between the iso-concentration surfaces to relate a triplet (OC4 maximum band ratio, $L_w(412)_N$, $L_w(555)_N$) to a chlorophyll concentration. On this grid, OC4 maximum band ratio varies from -0.5 to 2.8, $L_w(412)_N$ from -2.0 to 2.0 mW cm^{-2} nm^{-1} sr^{-1}, and $L_w(555)_N$ from 0.0 to 0.6 mW cm^{-2} nm^{-1} sr^{-1}.

Geometrical properties of the chlorophyll iso-concentration surfaces can be approached from scatterplots in different planes. Figure 6 presents OC4 maximum band ratio versus $L_w(412)_N$, whatever $L_w(555)_N$, for *in situ* data located in the English Channel and the Bay of Biscay. On that figure, we observe numerous negative $L_w(412)_N$ values and, at constant chlorophyll concentration, a trend to lower OC4 ratios when $L_w(412)_N$ decreases. Figure 7 presents OC4 ratio versus $L_w(555)_N$, whatever $L_w(412)_N$. We observe that, at constant concentration lower than about

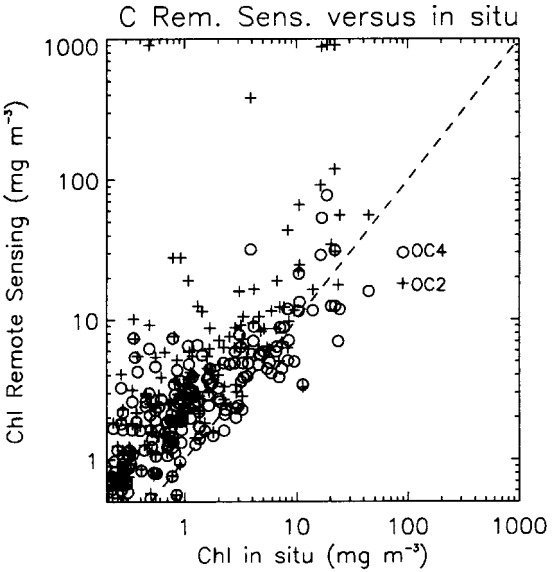

Figure 5. Comparison between chlorophyll-a concentrations derived from OC2 and OC4 models and *in situ* observations. Over-estimation appears at any level in chlorophyll concentration. Negative ratios (2 at 443/555 and 1 at 490/555) have been arbitrarily related to chlorophyll concentration $1000\,\mathrm{mg\,m^{-3}}$.

$10\,\mathrm{mg\,m^{-3}}$, OC4 ratio decreases as $L_w(555)_N$ increases. We can also conclude from that graph that there is a level in the OC4 ratio, around 0.7, which is observed for a large interval of chlorophyll concentrations. This level leads to a theoretical chlorophyll concentration of about $10\,\mathrm{mg\,m^{-3}}$ (see figure 4). Thus, it is not surprising to obtain such high concentrations when applying OC2 or OC4 to winter SeaWiFS scenes where the chlorophyll concentration is as low as $0.2\,\mathrm{mg\,m^{-3}}$. These latter situations are encountered in areas of high suspended matter concentration frequently observed in winter scenes.

Based on the behaviours apparent on figures 6 and 7, we parametrize the iso-concentration surfaces using six parameters. Two of them will be used to transform the band ratio reference values given by OC4 for case 1 water, three parameters will be employed to relate these modified OC4 reference values to the 412 nm water-leaving radiance, and the last parameter will be the negative term in the exponential curve relating concentration to the 555 water-leaving radiance. Though the estimated parameters do not result from an optimized minimization procedure, a large set of parameters have been tested and evaluated following their rms error, defined by equation (17).

$$\mathrm{RMS} = \sqrt{\frac{\sum_{i=1}^{n}\left[\frac{c_{\mathrm{est},i} - c_{\mathrm{obs},i}}{c_{\mathrm{obs},i}}\right]^2}{n}} \tag{17}$$

where $c_{\mathrm{est},i}$ is the estimated value of chlorophyll concentration corresponding to the ith observation $c_{\mathrm{obs},i}$.

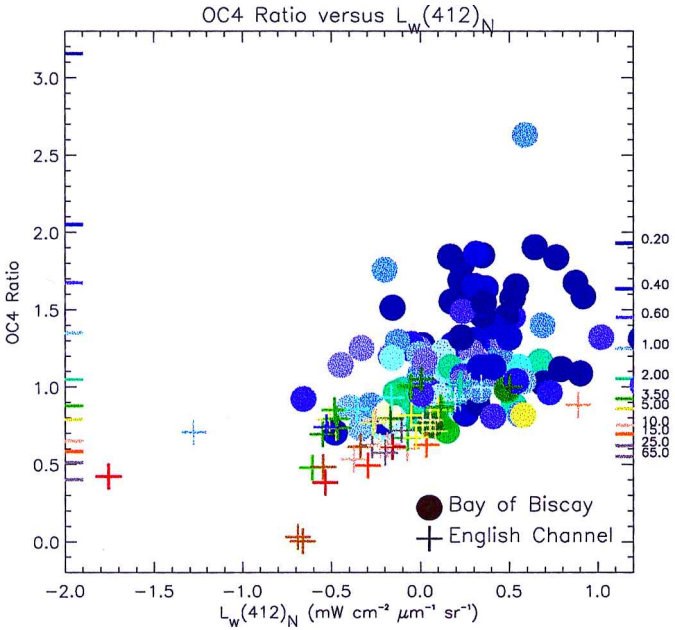

Figure 6. OC4 ratio versus the normalized water-leaving radiance at 412 nm for different classes of *in situ* chlorophyll a concentrations. Vertically on the left, coloured segments mark the OC4 SeaDAS4.0 theoretical ratio level. Same segments on the right mark the adjusted position.

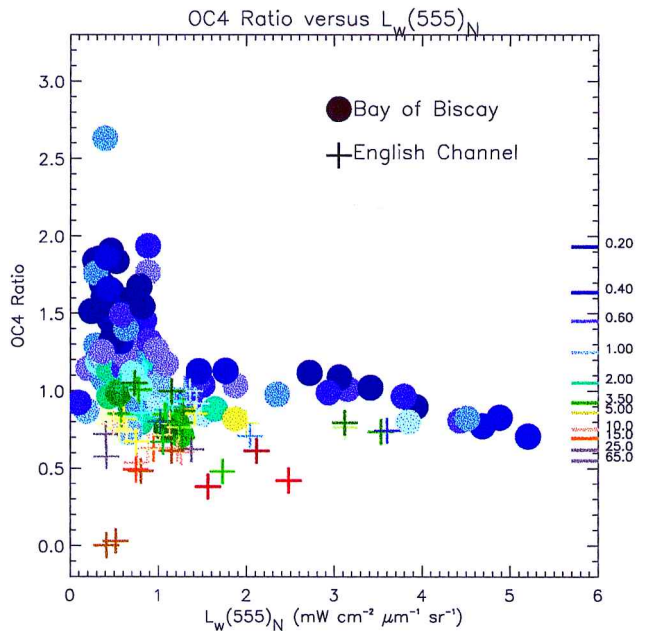

Figure 7. OC4 ratio versus the normalized water-leaving radiance at 555 nm for different classes of *in situ* chlorophyll a concentrations.

This rms is well suited for evaluating the performance of an algorithm applied to data ranging over three orders of magnitude, here from 0.2 to 60 mg m^{-3}. Nevertheless, we can only get an indication from such a parameter, which appears to be, like many others, very sensitive to the composition of the dataset, more or less well balanced in concentration. To choose the best parameter values, we will also consider the differences between means and medians of the experimental and estimated dataset.

6.1.1. *Modelling the OC4 ratio for clear water, characterized by high* $L_w(412)$*, at each concentration class*

It is already apparent from figure 4 that, for the low concentration measurements, the observed band ratios were lower than expected from the SeaDAS 4.0 OC4 curve. Figure 6 shows (vertically on the left) the theoretical OC4(C_I) ratio for each of the given concentration classes C_I (table 2). On the right vertical axis are shown new OC4 ratios adjusted for very clear water conditions, characterized in our scheme by high $L_w(412)$. These values are noted OC5$_a$(C_I), where the index a refers to their asymptotic character, as a function of $L_w(412)$ (see figure 8(*a*)). Two parameters A1 and A2, estimated respectively at 0.18 and 2.0, are used to modify the initial OC4(C_I).

$$OC5_a(C_I) = OC4(C_I) - A1(OC4(C_I) - 0.55)^{A2} \tag{18}$$

where OC4(C_I) is obtained following the formulation and coefficients given in O'Reilly *et al.* (1998) and used in SeaDAS 3.3.

From equation (18), as OC4(C_{65}) is equal to 0.55, OC5$_a$(C_{65}) = OC4(C_{65}). The reference ratio for 65 mg m^{-3} is thus unchanged.

We notice that this reference ratio OC4(C_{65}), visible on the right vertical axis of figure 6, is higher than that in SeaDAS 4.0 (left vertical axis). Nevertheless, this value appears as an upper bound which is rarely reached.

6.1.2. *Modelling the iso-concentration lines in the (OC4 band ratio,* $L_w(412)_N$*) plane*

Figure 8(*a*) shows the behaviour of the iso-concentration lines in the plane $L_w(555)_N = 0$. From right to left on the figure, the isoline $C_I(L_w(412)$ decreases from the level OC5$_a$(C_I) as soon as $L_w(412)_N$ is smaller than L (third estimated parameter) to finally reach R_I for $L_w(412)_{N\min} = -2.0$ mW cm^{-2} nm^{-1} sr^{-1}. The formulation of the curve OC5(C_I, ($L_w(412)_N$) was chosen in order to show a linear behaviour followed by a plateau.

$$\begin{aligned} OC5(C_I, L_w(412)_N) = &\{OC5_a(C_I) - OC5(C_I, L_w(412)_{N\min})\}(1.5h - 0.5h^3) \\ &+ OC5(C_I, L_w(412)_{N\min}) \end{aligned} \tag{19}$$

where $h = \{L_w(412)_N - L_w(412)_{N\min}\}/\{L - L_w(412)_{N\min}\}$ for $L_w(412)_N < L$ and $h = 1$ for $L_w(412)_N \geqslant L$; where $L = 1.0$ mW cm^{-2} nm^{-1} sr^{-1}.

OC5(C_I, $L_w(412)_{N\min}$) is the OC5 band ratio at the origin.

For any concentration I, OC5(C_I, $L_w(412)_{N\min}$) is defined from the values

Table 1. OC4 maximum band ratio.

Ratio	$R_{rsw}(443)/R_{rsw}(555)$	$R_{rsw}(490)/R_{rsw}(555)$	$R_{rsw}(510)/R_{rsw}(555)$
Highest ratios	7	24	147

Table 2. Central values and deviation (in $mg\,m^{-3}$) for data classes presented in figure 8.

Central value	0.25	0.4	0.6	1.0	2.0	3.5	5.0	10.0
Deviation	+0.05	±0.1	±0.1	±0.2	±0.5	±0.5	±1.0	±2.5

$OC5(C_{65}, L_w(412)_{Nmin})$ and $OC5(C_1, L_w(412)_{Nmin})$, for 65 and $1.0\,mg\,m^{-3}$, which are the next two parameters, using the following interpolation formula:

$$OC5(C_I, L_w(412)_{Nmin}) = \min(OC5_a(C_I), \frac{OC5_a(C_I) - OC5_a(C_{65})}{OC5_a(C_1) - OC5_a(C_{65})} \{OC5(C_1, L_w(412)_{Nmin}) - OC5(C_{65}, L_w(412)_{Nmin})\} + OC5(C_{65}, L_w(412)_{Nmin}) \quad (20)$$

$OC5(C_{65}, L_w(412)_{Nmin})$ and $OC5(C_1, L_w(412)_{Nmin})$ were set to -0.2 and 1.0 respectively.

6.1.3. *Modelling the iso-concentration lines in the (OC4 band ratio, $L_w(555)_N$) plane*

In the plane (OC4 ratio, $L_w(555)_N$) at a given $L_w(412)_N$, we model the iso-line $OC5(C_I)$ as a function of $L_w(555)_N$ by:

$$OC5(C_I, L_w(412)_N, L_w(555)_N) = e^{A3\,L_w(555)_N}\{OC5(C_I, L_w(412)_N) - OC5(C_{10}, L_w(412)_N)\} + OC5(C_{10}, L_w(412)_N) \quad (21)$$

where $OC5(C_{10}, L_w(412)_N)$ is the OC5 ratio for the iso-concentration line corresponding to $10\,mg\,m^{-3}$, for a given value of $L_w(412)_N$, and $A3 = -0.4$

Equation (21) will be applied to OC4 ratios greater than $OC5(C_{10}, L_w(412)_N)$. For ratios lower than $OC5(C_{10}, L_w(412)_N)$, $L_w(555)_N$ is no longer considered (see figures 7 and 8(*i*)). It is not surprising that $L_w(555)_N$ does not significantly affect the position of the iso-concentration line for high chlorophyll concentration. In eutrophic waters, $L_w(555)$ cannot be attributed significantly to suspended matter, as light is required for photosynthesis. It is more linked to the phytoplankton itself and its detrital product which is implicitly taken into account in the $OC5(C_I, L_w(412)_N)$ term.

6.2. *Application and comparison to cruise measurements*

The six parameters, described above, A1, A2, A3, *L*, $OC5(C_{65}, L_w(412)_{Nmin})$ and $OC5(C_1, L_w(412)_{Nmin})$, lead to iso-concentration surfaces and, after interpolation between these surfaces, to a table relating SeaWiFS triplets (OC4 maximum band ratio, $L_w(412)_N$ and $L_w(555)_N$) to chlorophyll concentration. For the adjusted set of parameters, the rms, defined in equation (17), is equal to 0.66, and the r^2 coefficient of the regression line, shown on figure 9, is equal to 0.70 for log-transformed data. The mean and the median of the estimated chlorophyll concentrations are equal to 3.18 and 1.04, compared with 3.35 and $0.95\,mg\,m^{-3}$ for the *in situ* reference set. The rms, approached by 66%, can be interpreted only as an indicator of the relative error as its statistics are not easily determined. On one hand, we should consider the fact that the calculated error is lower than the true rms as it is derived from a dataset already used to elaborate the formulation of the parametrization and to estimate the six parameters. On the other hand, a part of the scattering around the observed values can be related to the geophysics itself, through the spatial distribution of the samplings within a pixel area and the temporal variability within a day.

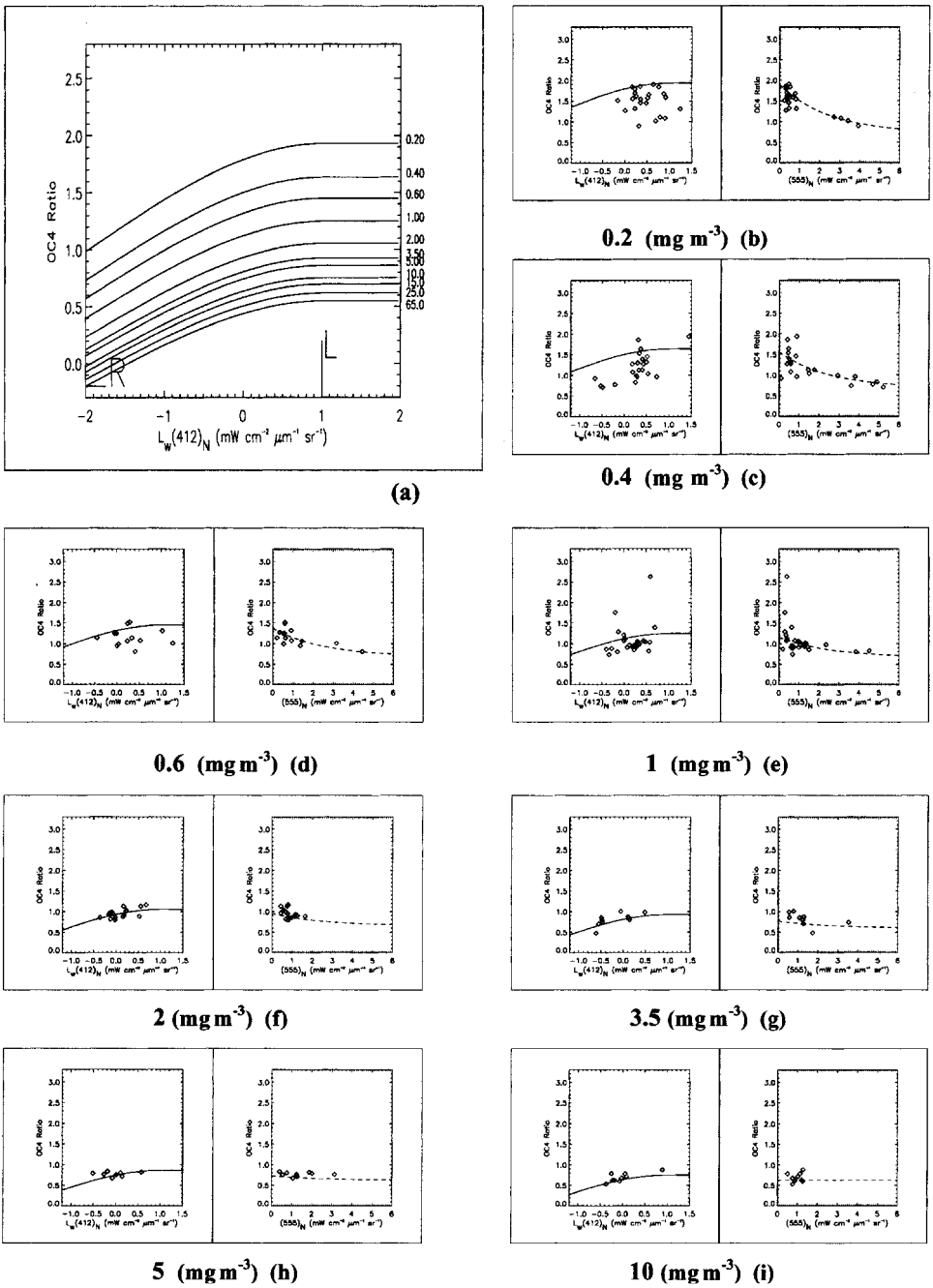

Figure 8. Chlorophyll a concentrations in the (OC4 ratio, $L_w(412)_N$, $L_w(555)_N$) space and parametrized iso-concentration curves. (*a*) Section at $L_w(555)_N = 0$. Curves and scatter plots for different concentration classes: for each class, left curve shows OC4 ratio versus $L_w(412)_N$ for $L_w(555) = 0$; right curve shows OC4 ratio versus $L_w(555)_N$ for $L_w(412)_N$ equal to the mean of the data in the class. (*b*) 0.2, (*c*) 0.4, (*d*) 0.6, (*e*) 1.0, (*f*) 2.0, (*g*) 3.5, (*h*) 5.0, (*i*) 10.0 mg m^{-3}.

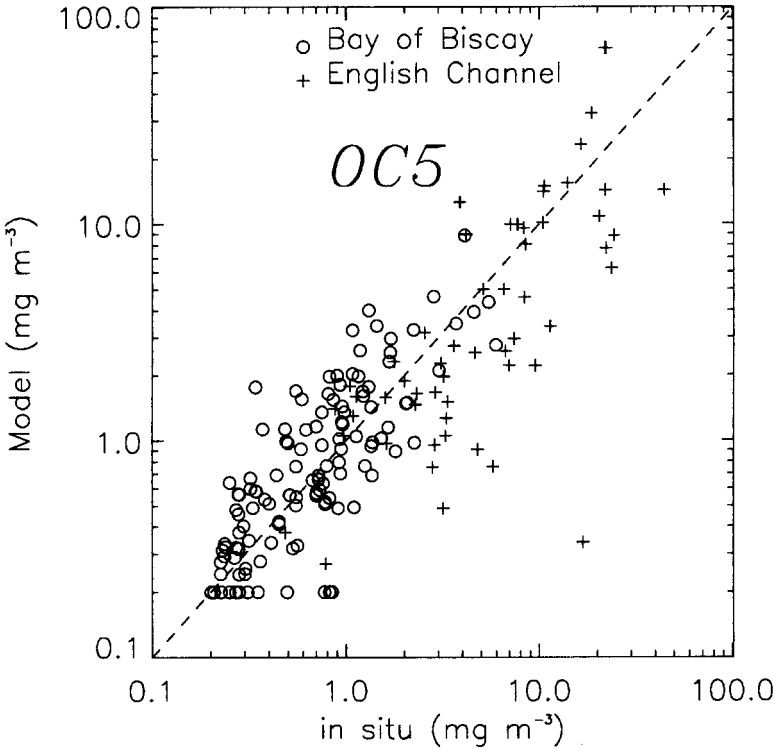

Figure 9. Scatterplots of estimated versus *in situ* chlorophyll a concentrations, $r^2 = 0.70$ for log-transformed data.

On figure 9, one point, corresponding to a concentration of 16.5 mg m^{-3}, appears to be under-estimated by our algorithm as the retrieved value is only 1.5 mg m^{-3}. This point has been measured at the boundary of the plume of the Seine in May, in a frontal area subject to significant displacement with the tidal currents. This shows how difficult the calibration of ocean colour algorithms is in coastal waters.

More details are presented in figure 8 for the different classes of observed chlorophyll concentrations. The scatterplots of OC4 maximum band ratio versus $L_w(412)_N$ and $L_w(555)_N$, and the fitted iso-lines are also presented in this figure. For low concentrations, 0.2 or 0.4 mg m^{-3}, the dispersion in $L_w(555)_N$ appears to be very strong. These data correspond to cruises made in the Bay of Biscay during winter. Froidefond *et al.* (accepted) attribute the over-estimation of chlorophyll concentration by OC4 at that period to the effect of a high load in suspended particulate matter, mostly due to bottom resuspension. The over-estimation can be explained by an increase in $L_w(555)N$ and a consequent decrease in the ratios. By looking at figure 8(*c*), we observe that, for that low concentration classes, the lowest OC4 ratios are obtained for triplets showing highest $L_w(555)_N$ and lowest $L_w(412)_N$. Applying OC2 or OC4 algorithms to that kind of data would provide estimates of the chlorophyll concentration ten times superior to reality.

Though coincident *in situ* and satellite data are scarce from late summer to spring, figure 10 shows the impact of the modified OC4 algorithm on the estimation of the chlorophyll concentration. Figure 10(*a*) presents the SeaWiFS scene corresponding to the Biomet2 cruise, a typical winter situation in the Bay of Biscay,

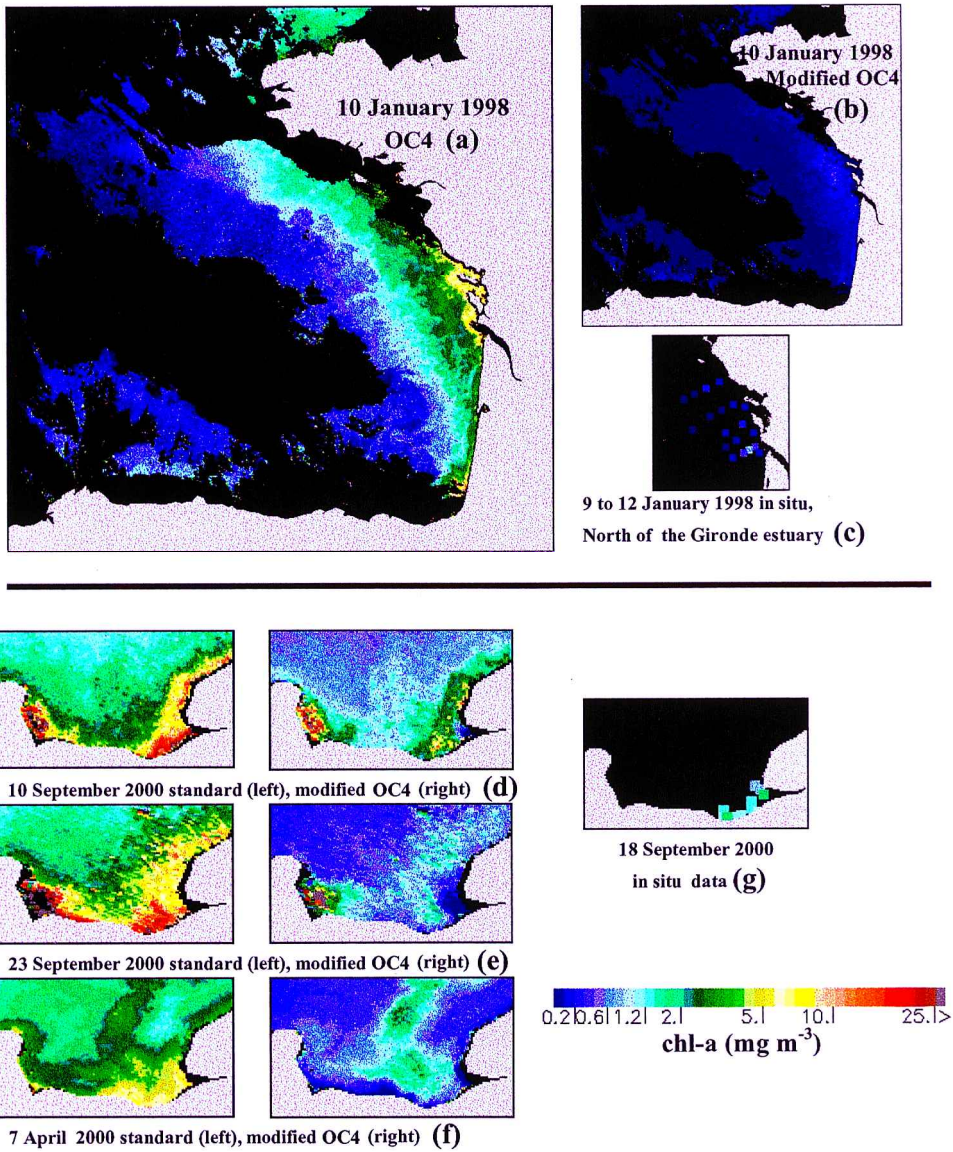

Figure 10. Effect of the modified algorithm on the retrieved chlorophyll concentration from late summer to early spring. The contrast between standard (OC4 images on the left) and modified algorithms (images on the right) is very high for that period of the year. (*a*) 10 January 1998 OC4, (*b*) 10 January 1998 modified OC4, (*c*) 9–12 January 1998 *in situ*, north of the Gironde Estuary. Standard (left) and modified (right) OC4 for (*d*) 10 September 2000, (*e*) 23 September 2000, (*f*) 7 April 2000. (*g*) 18 September 2000, *in situ* data. *In situ* data of the biomet2 cruise (*c*), show good agreement with the estimates derived from the modified OC4 (*b*). In the presence of a high load of suspended matter in water, OC4 (*a*) and left of (*d*), (*e*), and (*f*), over-estimate the chlorophyll concentration.

processed by standard OC4. Our five channel algorithm reduces the estimates of chlorophyll dramatically (see figure 10(*b*) and (*c*)).

On a series of images on the Bay of Seine presented in figure 10(*d*)±(*g*), only selected because of clear skies, the chlorophyll concentration is dramatically diminished by application of the modified OC4. Though we have no coincident satellite—*in situ* pairs of data in the Bay of Seine on 18 September 2000, measured *in situ* data (*g*), show a better agreement with the modified than with the standard OC4 estimates on 10(*d*) and 23 September (*e*), the latter appearing too high. Another clear image, at the beginning of April in the Bay of Seine (*f*), shows chlorophyll concentrations derived from the modified OC4 very close to what is expected, the peak in chlorophyll being outside the plume.

The estimation derived from the standard OC4 algorithm are so far from the expected reality in autumn and winter that biologists may be reluctant to use the SeaWiFS imagery, though the quality of the estimations in spring and summer when the optical properties of coastal waters, dominated by chlorophyll pigments, approach those of case 1 waters. By applying our modified algorithm, we derived a coherent set of chlorophyll concentration all over the year.

For chlorophyll-poor water, the decrease in retrieved chlorophyll concentration appearing in our procedure is due to the $L_w(555)_N$ correction. At higher concentration, the $L_w(412)_N$ correction, shown in figure 8(*a*), becomes more and more significant. Negligible for chlorophyll concentrations near $5\,mg\,m^{-3}$ the $L_w(555)_N$ correction is assumed zero for concentrations superior to $10\,mg\,m^{-3}$. For such concentrations, the $L_w(412)_N$ correction becomes significant as the retrieved concentration is very sensitive to small variations in the OC4 ratio.

Figure 11 presents a situation in the Bay of Seine corresponding to high concentrations in chlorophyll. A significant set of data was obtained during a SeaWiFS dedicated cruise, carried out from the IFREMER station of Port en Bessin, as soon as the weather conditions were favourable. The confidence is very high in the retrieved concentrations shown in figure 11(*a*) and (*b*). The decrease in chlorophyll concentration along the southern shores of England and around the Island of Wight is substantial. Nevertheless, we have no data to draw a definitive conclusion from such a correction.

Many situations in spring and summer in the Bay of Biscay show good agreement between the standard and modified OC4 algorithms. The retrieved concentrations (using both standard or modified algorithms), not shown, fit perfectly the patterns and levels encountered during the Biomodycot-2 cruise in June 1999. Contrary to most of the autumn and winter situations, higher values can sometimes be retrieved from our modified algorithm in spring and summer. This result can be explained by the fact that the radiances at 412 nm are high and the chlorophyll concentrations significant (see figure 6 to compare the ratios used in standard and modified OC4 algorithms at high 412 radiance).

7. Conclusion

Our major focus was to provide to biologists the means to derive reliable chlorophyll concentrations from the SeaWiFS radiances derived from the standard SeaDAS procedure. Aiming to produce regular estimations at all seasons, we have encountered very distinct water types, from winter waters, related to the worst case 2 types, to spring situations when the primary production flourishes. We did not aim to develop a new concept in ocean colour techniques, such as OC2 or OC4 or others, which

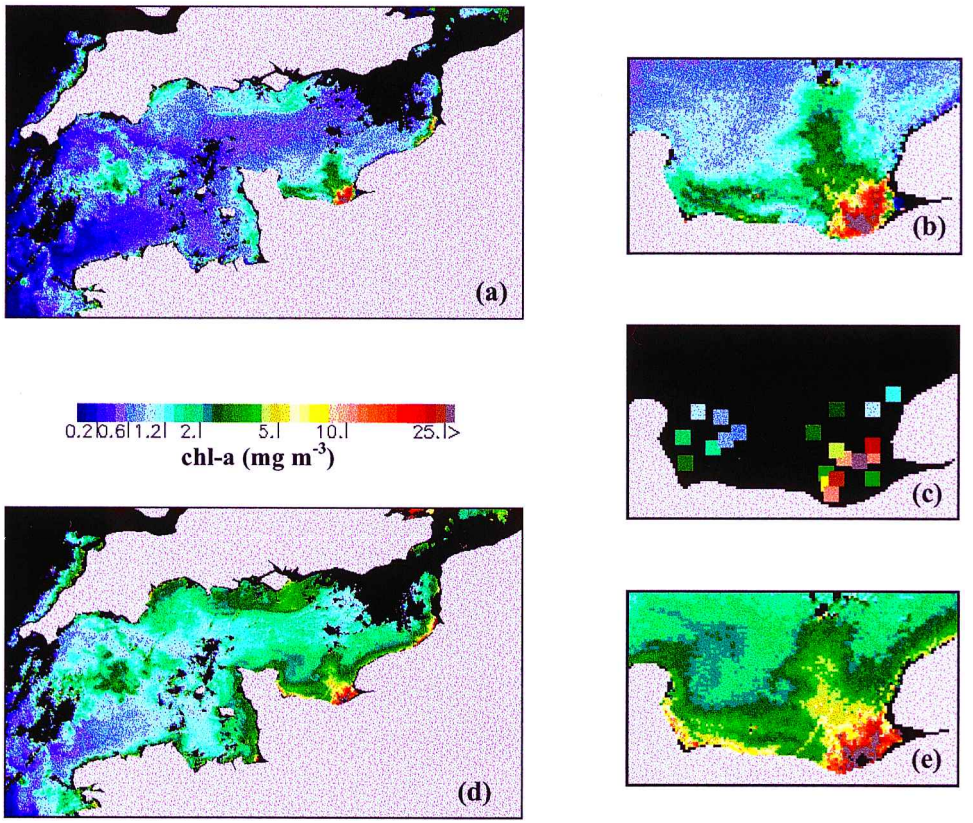

Figure 11. The surface chlorophyll content during the SEINESAT cruise from 30 August to 2 September. (*a*) Modified OC4 on 1 September 1999 at 12h30 UT over the English Channel. (*b*) Zoom on the Bay of Seine. (*c*) *In situ* measurements from 30 August to 2 September 1999. Standard OC4 applied to the whole SeaWiFS scene (*d*) and zoom on the Bay of Seine (*e*).

would have imposed a specific *in situ* instrumentation and duplicated research already carried out by other teams, most of them involved in the MODIS and MERIS calibration and validation projects. Our object was only to define a lookup table, which can be easily applied to SeaWiFS data processed by the standard SeaDAS routines, to obtain a consistent series of chlorophyll concentration. In coastal areas, considering the limited set of channels available from SeaWiFS, the atmospheric correction will remain a difficult task which will require specific and regional investigations. Advanced algorithms, simultaneously providing atmospheric correction and retrieval of the optical properties of the water, propose iterative procedures for the inversion of the atmosphere–ocean radiative transfer model through different means, among them, neural network algorithms or genetic programming. These latter techniques are very promising but still under development at this time.

The limitation of the current SeaDAS Version 4.0 procedure is clearly detected where the water-leaving radiance is negative. However, as long as the atmospheric correction scheme continues to provide regular products, 'robust' in the sense that they are not submitted to strong dependencies on regional atmospheric and oceanic fluctuations, negative values are acceptable. The six parameters that we have introduced in our

scheme refer to very distinct aspects in the parametrization of the iso-concentration surfaces and they can be easily modified to take into account any future progress in the OC4 formulation or in the atmospheric correction (lower slopes in the OC4 ratio-radiance at 412 nm are expected from an improved atmospheric correction procedure). In the near future, new data will certainly lead to a new lookup table relating the satellite triplets to the chlorophyll concentration. Whatever the future results expected, the biologists will find with SeaWiFS data processed by SeaDAS a unique and considerable source of information for their research, even in coastal areas.

Acknowledgments

The authors would like to thank the SeaWiFS Project and the Distributed Active Archive Center at the Goddard Space Flight Center, Greenbelt, Maryland, for the production and distribution of the SeaWiFS data acquired at the Dundee and Roma stations. We are also indebted to NASA for providing the SeaDAS software. We are extremely grateful to all who provided the field measurements: J.F. Chiffoleau (BloomSeine, Marina 8, CadHiver), the IFREMER's group of Port-en-Bessin (SeineSat), V. Duquesne (SRN), J.M. Froidefond (Biomet), S. L'Helguen and N. Savoye (Bloom/QuickSeine), A. Herbland and C. Labry (Plagia), T. Labasque (Modycot.99), S. Loyer and P. Cann (Ecoloire). The authors thank Olivier Archer for providing useful tools to visualize SeaWiFS scenes and field data.

The lookup table is available on request to the authors (Francis.Gohin@ifremer.fr). An IDL routine can be provided to read the table for deriving estimates of the chlorophyll-a concentration from level-2 SeaDAS channels.

Appendix

Table A1. Statistics of the *in situ* data (mg m^{-3}).

Area	English Channel	Bay of Biscay	Total
Number of measurements	56	122	178
Mean	8.36	0.94	3.27
Median	5.12	0.76	0.95
Higher value	44.43	5.96	44.43
Lower value	0.48	0.20	0.20

Table A2. Temporal distribution of the *in situ* data numbers.

Cruise	Jan	Feb	Mar	Apr	May	Jun	Jul	Aug	Sep
Eng. Channel									
SRN		2	3	2	2	3		2	
Quick/Bloom					4				
BloomSeine					1				
Marina					3				
CadHiv	2								
SeineSat 1999								6	16
SeineSat 2000						10			
Bay of Biscay									
Plagia		2		3	9	13	1		
Ecoloire							10		
Biomet2&3	12		12						
Modycot99-1				14					
Modycot99-2						15			
Modycot99-3									16
Modycot2000			15						

The pigment analysis of the MODYCOT cruises, in the Bay of Biscay, was made using HPLC. One-litre seawater samples were pre-filtered through 200 μm mesh nylon gauze and then filtered onto 25 mm GF/F fibre filters under low-pressure vacuum (<0.5 bar, following Del Amo *et al.* 1997) for further HPLC analysis. Filters were stored immediately at -20°C on board for the duration of the cruise and were kept in the laboratory for a maximum of 7 months at -80°C. Pigments were extracted and analysed by the reverse-phase HPLC method slightly modified from Wright *et al.* (1991). The frozen GF/F filters were ground and sonicated into 3 ml of acetone-water (90/10, v/v). For each sample, 500 μl of acetone-water extract were mixed with 165 μl IP solution and 35 μl of trans-canthaxanthin (internal standard) and 100 μl were injected automatically by a refrigerated (4° C) automatic sampler Thermo AS3000 in a ODS2 C18 column (150 mm × 4.6 mm, with 3 μm silica particles). The Thermo UV3000 detector scanned the range spectrum between 400 and 700 nm, and the effective detection was performed at 440 nm.

For the other cruises, chlorophyll a seawater content was measured using spectophotometric analysis. Seawater samples of 500 ml were filtered on to 47 mm GF/F fibre filters under low-pressure vacuum (<0.5 bar, following Del Amo *et al.* 1997) and grinding in acetone-water (90/10, v/v). The acetone extract, after centrifugation, was scanned at 665 nm and 750 nm on a Shimadzu UV-2401PC recording spectrophotometer. The concentration of chlorophyll a and pheopigments were determined using the acid spectrophotometric equations of Lorenzen (1967).

Table A3. Water-leaving radiance and solar irradiance for the eight SeaWiFS channels.

Band	Wavelength (nm)	Solar irradiance F_0 (μW cm^{-2} nm^{-1})
1	402–422	170.79
2	433–453	189.44
3	480–500	193.68
4	500–520	188.36
5	545–565	185.40
6	660–680	153.39
7	745–785	122.51
8	845–885	99.02

References

Antoine, D., and Morel, A., 1999, A multiple scattering algorithm for atmospheric correction of remotely sensed ocean colour (MERIS instrument): principle and implementation for atmospheres carrying various aerosols including absorbing ones. *International Journal of Remote Sensing*, **20**, 1875–1916.

Carder, K. L., Chen, F. R., Lee, Z. P., Hawes, S. K., and Kamykowski, D., 1999, Semianalytic Moderate-Resolution Imaging Spectrometer algorithms for chlorophyll *a* and absorption with bio-optical domains based on nitrate-depletion temperatures. *Journal of Geophysical Research*, **104**, 5403–5421.

Carder, K. L., Hawes, D. K., Baker, K. A., Smith, R. C., Steward, R. G., and Mitchell, B. G., 1991, Reflectance model for quantifying chlorophyll a in the presence of productivity degradation products. *Journal of Geophysical Research*, **96**, 20 599–20 611.

Carder, K. L., Reinersman, P., Chen, R., Muller-Karger, F., Davis, C., and Hamilton, M., 1993, AVIRIS calibration and application in coastal oceanic environments. *Remote Sensing of Environment*, **44**, 205–216.

Del Amo, Y., Queguiner, B., Treguer, P., Breton, H., and Lambert, L., 1997, Impacts of high-nitrate freshwater inputs on macrotidal ecosystems. II. Specific role of the silicic

acid pump in the year-round dominance of diatoms in the Bay of Brest (France). *Marine Ecology Progress Series*, **161**, 225–237.

FROIDEFOND, J. M., LAVENDER, S., LABORDE, P., HERBLAND, A., and LAFON, V., 2000, SeaWiFS data interpretation in a coastal area in the Bay of Biscay, accepted in *International Journal of Remote Sensing*.

FU, G., BAITH, K. S., and MCCLAIN, C. R., 1998, SeaDAS: The SeaWiFS data analysis system. *Proceedings of the 4th Pacific Ocean Remote Sensing Conference, Qingdao, China, 28–31 July*, edited by Ming-Xia He and Ge Chen (Beijing: Beijing Fortune Quick Printing Corporation), pp. 73–77.

GORDON, H. R., 1999, MODIS Normalized Water-leaving Radiance Algorithm Theoretical Basis Document (MOD 18) Version 4, Under Contract Number NAS5-31363, MODIS Web, http://modis.gsfc.nasa.gov/MODIS/ATBD/#OCEANS

GORDON, H. R., and CLARK, D. K., 1981, Clear water radiances for atmospheric correction of coastal zone colour scanner imagery. *Applied Optics*, **20**, 4175–4180.

GORDON, H. R., CHOMKO, R., and MOULIN, C., 2000, Advanced atmospheric correction algorithms, Ocean Optics CD-Rom, Musée Océanographique, Monaco, 16–20 October, Office of Naval Research, Ocean, Atmosphere, and Space Department.

GORDON, H. R., CLARK, D. K., MUELLER, J. L., and HOVIS, W. A., 1980, Phytoplankton pigments derived from the Nimbus-7 CZCS: Initial comparisons with surface measurements. *Science*, **210**, 63–66.

GORDON, H. R., and WANG, M., 1994, Retrieval of water-leaving radiance and aerosol optical thickness over the oceans with SeaWiFS: a preliminary algorithm. *Applied Optics*, **33**, 443–452.

HOOKER, S. B., ESAIAS, W., FELDMAN, E., GREGG, W. W., and MCCLAIN, C. R., 1992, An overview of SeaWiFS and Ocean Colour. NASA Tech. Memo 104566, Vol. 1, edited by S. B. Hooker and E. R. Firestone, NASA Goddard Space Flight Center, Greenbelt, Maryland.

HU, C., CARDER, K. L., and MULLER-KARGER, F., 1998, Preliminary algorithm to derive chlorophyll pigment concentration and DOM absorption in turbid coastal waters from SeaWiFS imagery. *Proceedings of the 4th Pacific Ocean Remote Sensing Conference, Qingdao, China, 28–31 July*, edited by Ming-Xia He and Ge Chen (Beijing: Beijing Fortune Quick Printing Corporation), pp. 78–82.

LORENZEN, C. J., 1967, Determination of chlorophyll and pheopigments: spectrophotometric equations. *Limnology and Oceanography*, **12**, 343–346.

MOORE, G. F., AIKEN, J., and LAVENDER, S. J., 1999, The atmospheric correction of water colour and the quantitative retrieval of suspended particulate matter in case II waters: application to MERIS. *International Journal of Remote Sensing*, **20**, 1713–1733.

MOREL, A., and BRICAUD, A., 1981, Theoretical results concerning light absorption in a discrete medium and application to specific absorption of phytoplankton. *Deep Sea Research*, **28**, 1375–1393.

MOREL, A., and PRIEUR, L., 1977, Analysis of variations in ocean colour. *Limnology and Oceanography*, **22**, 709–722.

O'REILLY, J. E., MARITORENA, S., MITCHELL, B. G., SIEGEL, D. A., CARDER, K. L., GARVER, S. A., KAHRU, S. A., and MCCLAIM, C., 1998, Ocean colour chlorophyll algorithms for SeaWiFS. *Journal of Geophysical Research*, **103**, 24 937–24 953.

SATHYENDRANATH, S., and PLATT, T., 1997, Analytic model of ocean colour. *Applied Optics*, **36**, 2620–2629.

SIEGEL, D., WANG, M., MARITORENA, S., and ROBINSON, W., 2000, Atmospheric correction of satellite ocean colour imagery: The black pixel assumption. *Applied Optics*, **39**, 3582–2591.

WRIGHT, S. W., JEFFREY, S. W., MANTOURA, R. F., LLEWELLYN, C. A., BJOERNLAND, T., REPETA, D., and WELSHMEYER, N., 1991, Improved HPLC method for the analysis of chlorophylls and carotenoids from marine phytoplankton. *Marine Ecology Progress Series*, **77**, 183–196.